Journal of Nano- and Electronic Physics
Vol. **11** No 4, 04026(5pp) (2019)

Журнал нано- та електронної фізики
Том **11** № 4, 04026(5cc) (2019)

Elastic Properties of Au, Ag, and Core-shell Au@Ag Nanorods from Molecular Dynamics Simulations

U. Shvets, B. Natalich, V. Borysiuk*

Sumy State University, 2, Rimsky-Korsakov St., 40007 Sumy, Ukraine

(Received 07 May 2019; revised manuscript received 02 August 2019; published online 22 August 2019)

We report the computational study of mechanical properties of gold, silver and core-shell Au@Ag nanorods. The dynamical behavior of the samples under tensile deformation was studied within classical molecular dynamics simulation. Interactions between atoms in the samples were described within embedded atom method (EAM) and EAM alloy model for gold – silver interaction in core-shell Au@Ag nanorod. To study the mechanical properties of the nanorods, the tensile deformation procedure was applied to the samples. Stretching of the samples was simulated by displacement of the fixed atoms located in the two external atomic layers at the opposite edges of the samples from each other at constant strain rate of 0.004 ps^{-1}. Temperature of the samples was maintained at 300 K using the Berendsen thermostat through the total simulation time. During the deformation process, mechanical stresses were calculated according to virial theorem for each sample and strain-stress curves were built from obtained data. Obtained strain-stress curves have typical shape with a linear section at the beginning and a further nonlinear part corresponding to plastic deformation. Young moduli of the studied samples were estimated through linear regression of the elastic part of the strain-stress curves. The obtained values are equal to 57.3 GPa, 80.1 GPa and 70.9 GPa for Au@Ag, Au and Ag samples, respectively. Analysis of the snapshots of atomistic configurations shows that considered samples are characterized by different failure dynamics, namely necking was observed only for Au@Ag core-shell nanorod, while pristine gold and silver samples are characterized by failure without clearly visible necking. Comparative analysis of the obtained results shows a good agreement with the similar data available in the literature.

Keywords: Molecular dynamics, Nanorod, Core-shell, Young modulus.

DOI: 10.21272/jnep.11(4).04026 PACS numbers: 02.70.Ns, 62.25. – g

1. INTRODUCTION

Metallic nanowires and nanorods of different chemical compositions and structures are very promising materials that are widely investigated as potential materials for components of various nanoelectronic devices [1, 2]. Among different possible geometrical shapes and forms, nanoparticles with core-shell structure are one of the most studied bimetallic materials. Such objects can be synthesized and designed by various chemical methods [2, 3].

Experimental investigation of the nanosized object is a very complicated task, and, besides that, data obtained from experiments usually needs further analysis. Moreover, such studies require very expensive equipment and technologies. Alternative approaches of such investigations are studies by theoretical and computational methods. One of possible options of theoretical approaches is molecular dynamics (MD) simulation which is effective and precise enough method for computational study of the structural and mechanical properties of nanomaterials [4, 5]. In the present work we report the MD study of the elastic properties of gold, silver and bimetallic gold-silver nanorod with core-shell structure.

2. MODEL AND SIMULATION SETUP

During the simulation of deformation processes of metallic nanowires, the interactions between atoms were described using the embedded atom method (EAM) [6]. EAM approach is widely used in the simulation of metal alloys by classical MD techniques and is known to realistically reproduce the basic properties of metals such as lattice constant, interatomic distance, energy of interaction between atoms and others.

Within the EAM, the total potential energy of a metallic crystal can be presented as a sum of two components, each of which describes the corresponding mechanisms of interaction:

$$U = \frac{1}{2}\sum_{i,j,i\neq j}\varphi(r_{ij}) + \sum_i F(\rho_i), \quad (1)$$

where $\varphi(r_{ij})$ is the pair energy between atoms i and j at a distance r_{ij}; $F(\rho_i)$ is the local embedding energy of the i-atom in the space domain, that is characterized by the electronic density ρ_i.

For each term in equation (1), the analytical expression was proposed through approximating the data obtained from the calculations from the first principles [6]. Thus, the pair energy of the interatomic interaction can be written in the form

$$\varphi(r) = \frac{A\cdot\exp\left[-\alpha\left(\frac{r}{r_e}-1\right)\right]}{1+\left(\frac{r}{r_e}-\kappa\right)^{20}} - \frac{B\cdot\exp\left[-\beta\left(\frac{r}{r_e}-1\right)\right]}{1+\left(\frac{r}{r_e}-\lambda\right)^{20}}, \quad (2)$$

where r_e is the equilibrium distance between the two atoms of the given type; A, B, α, β are the approximation parameters; κ, λ are the additional parameters for

* v.borisyuk@phe.sumdu.edu.ua

ensuring zero energy of interaction at significant interatomic distances.

The local embedding energy as a function of electron density $F(\rho_i)$ is calculated in several steps. Firstly, the electronic density ρ_i is calculated as

$$\rho_i = \sum_{i,j\neq i} f\left(r_{ij}\right), \tag{3}$$

where $f(r_{ij})$ is the local electron density in the atomic region of atom i calculated through the following expression

$$f\left(r\right) = \frac{f_e \cdot \exp\left[-\beta\left(\frac{r}{r_e}-1\right)\right]}{1+\left(\frac{r}{r_e}-\lambda\right)^{20}}, \tag{4}$$

that has the same form as the second term in formula (2) with the same values of parameters β and λ. Then, the electronic density function $F(\rho_i)$ should be calculated from three following equations depending on the value of ρ_i

$$F\left(\rho\right) = \sum_{i=0}^{3} F_{ni}\left(\frac{\rho}{\rho_n}-1\right)^i, \quad \rho < \rho_n, \quad \rho_n = 0{,}85\rho_e, \tag{5}$$

$$F\left(\rho\right) = \sum_{i=0}^{3} F_{i}\left(\frac{\rho}{\rho_e}-1\right)^i, \quad \rho_n \le \rho < \rho_0, \quad \rho_0 = 1{,}15\rho_e, \tag{6}$$

$$F(\rho) = F_e\left[1-\ln\left(\frac{\rho}{\rho_e}\right)^{\eta}\right]\cdot\left(\frac{\rho}{\rho_e}\right)^{\eta}, \quad \rho_0 \le \rho. \tag{7}$$

Such method for determining the electronic density function $F(\rho_i)$ is necessary for the realistic approximation of the embedding energy and for reproducing the properties of the material in a wide range of values ρ.

The forces between different types of atoms can be calculated using the EAM model for alloys [6]. Within mentioned approach, the pair energy $\varphi^{ab}(r_{ij})$ between atoms of type a i b can be calculated as

$$\varphi^{ab}(r) = \frac{1}{2}\left(\frac{f^b(r)}{f^a(r)}\varphi^{aa}(r) + \frac{f^a(r)}{f^b(r)}\varphi^{bb}(r)\right). \tag{8}$$

Analytical expressions and numerical parameters for the functions used in expressions (1)-(8) for several metals can be found in the paper [6].

It should be noted that the complete algorithm for particle motion calculations used in MD simulations involves obtaining analytical expressions for the forces of interatomic interaction $F(r_{ij})$ based on the given dependences for the potential energy through the equation

$$F(r) = -\frac{\partial U}{\partial r} \tag{9}$$

and further numerical integration of the equations of motion

$$\frac{d^2 r_i}{dt^2} = F_i(r_i) = -\frac{\partial U}{\partial r}, \tag{10}$$

for each atom i.

Thus, using equations (1)-(10), it is possible to investigate the dynamics of metallic nanorods under the external influences.

In this paper, we study the mechanical parameters of gold, silver and bimetallic nanowire with the core (Au) – shell (Ag) structure during deformation under the external load. In addition to the deformation of Au@Ag sample [7, 8], we also consider pristine Au and Ag samples under tensile deformation with calculation of strain-stress curves and tracking the dynamics of failure. From these dependences, the Young moduli for each sample were calculated. Also, during the simulation the instant atomistic configurations of the samples were obtained during the deformation process.

The choice of chemical composition of the nanowire investigated in the paper is caused by the fact that gold and silver are well combined in various compounds, since they have face-centered cubic crystal lattices with constants $a_{Au} = 0.4078$ nm, $a_{Ag} = 0.4086$ nm, respectively. Moreover, different types of Au–Ag nanostructures are widely used in nanoelectronics and can be obtained by different methods [1, 2, 9].

We consider a bimetallic Au–Ag nanowire with a core-shell structure and a cylindrical shape, with a length-to-diameter ratio of 2. Such choice of the geometric form of the objects under study is due to the need to avoid undesirable size effects [4]. The length of the nanowire is 8 nm, the diameter of the inner part (core) is 1.5 nm. The initial atomistic configuration of the investigated nanowire is shown in Fig. 1.

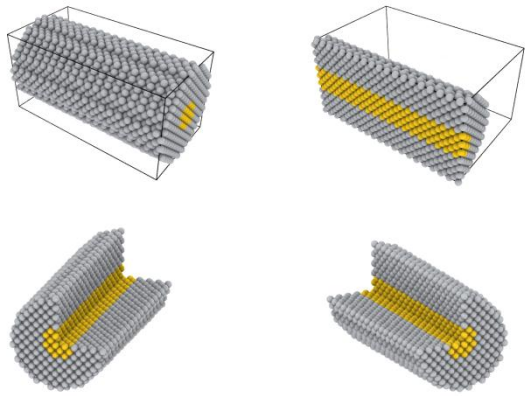

Fig. 1 – Initial atomistic configuration of Au@Ag core-shell nanowire. Overall view (top left), cross section (top right) and segments (bottom panel)

In initial configuration of the sample, the atoms of gold and silver were placed in the nodes of a face-centered cubic lattice with corresponding values of a solid lattice. The distances between atoms in the two external atomic layers on each of the cylinder bases were fixed to prevent relaxation during deformation and to provide appropriate boundary conditions.

In order to study the dynamical behavior of the sys-

tem under tensile load, a stretching procedure was applied to the sample, during which the strain-stress dependencies were calculated.

Simulation of the external load was carried out in the following way: displacement at a constant speed of 0.004 ps^{-1} was applied to fixed atoms located in the two external atomic layers at the opposite edges of the cylinder. The displacement was directed so that the opposite bases of the cylinder gradually moved from each other to simulate stretching of the samples.

During the deformation of the sample, mechanical stresses were calculated using the virial theorem [10], as

$$\sigma_{ij} = \frac{1}{V}\sum_{\alpha=1}^{N}\left(\frac{1}{2}r_{\alpha\beta}^{i}f_{\alpha\beta}^{j} - m^{\alpha}v_{i}^{\alpha}v_{j}^{\alpha}\right), \qquad (11)$$

where i, j are the Cartesian coordinates; α, β are the atom indexes; $r_{\alpha\beta}^{i}$, $f_{\alpha\beta}^{j}$ are the corresponding vector components of distances and forces between atoms α and β; m is the atomic mass; V – is the volume of sample.

Thus, by calculating the corresponding components of velocities and forces of interatomic interaction at the given strain ε, one can obtain the strain-stress curve $\sigma(\varepsilon)$.

During simulation, the temperature of the samples was maintained at $T = 300$ K using the Berendsen thermostat [11].

3. RESULTS AND DISCUSSION

To study the mechanical properties of bimetallic Au–Ag nanorod, the numerical procedure of simulation of stretching described above was performed and the corresponding strain-stress curves and instantaneous atomistic configurations of the system were calculated. Dependence of mechanical stresses on deformation is shown in Fig. 2.

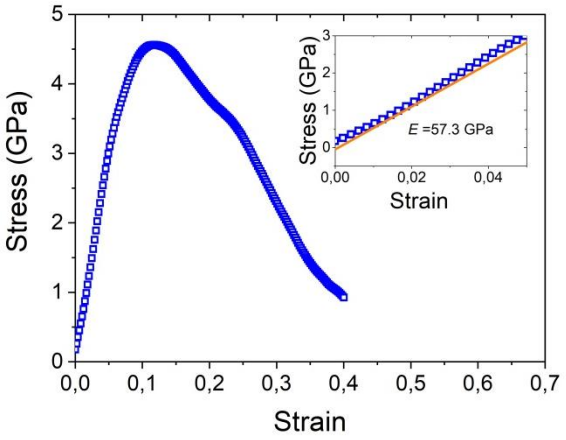

Fig. 2 – Strain-stress curve for bimetallic Au@Ag nanowire. The inner panel shows an enlarged plot of the elastic part with a linear approximation

It can be seen from Fig. 2 that the obtained strain-stress curve has a typical shape with a linear section at the beginning and a further nonlinear part corresponding to plastic deformation. The point with the maximum value of stress corresponds to the strength limit, after which the sample undergoes plastic deformation with subsequent destruction. The critical value of mechanical stress, after which the sample undergoes plastic deformation, corresponds to the strain value $\varepsilon \geq 0.1$. Linear interpolation of the elastic part of strain-stress curve gives the value of Young modulus $E = 57.3$ GPa for Au@Ag sample.

Atomistic configurations of the nanorod during tensile deformation are shown in Fig. 3.

As can be seen from the figure, after the point corresponding to the strength limit, the area with the formation of fragments with plastic deformation becomes noticeable within the sample. In this case, the Au–Ag nanowire retains the core-shell structure in the most part of the sample during plastic deformation and further fracture.

To validate the obtained results, the simulation models of the pristine gold and silver nanorods were also built, with the aim to compare quantities calculated from simulation with similar data available in literature. To obtain reliable data, a widely used simulation package LAMMPS [12] was used for simulations of the Au and Ag nanorods, under the similar conditions as Au@Ag core-shell nanorod.

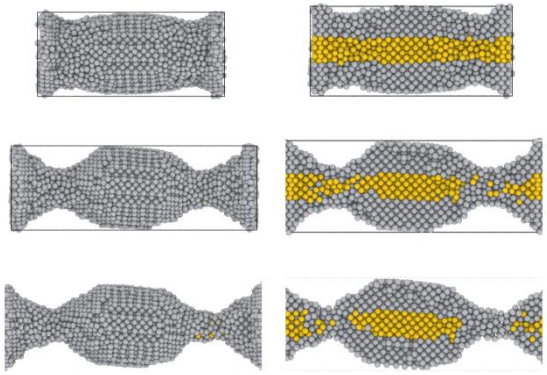

Fig. 3 – Atomic configurations of Au–Ag nanowire at strain of 15 %, 30 % and 60 % from top to bottom. General view (left) and cross-section (right)

Strain-stress curves obtained from MD simulations for Au and Ag nanorods are shown in Fig. 4.

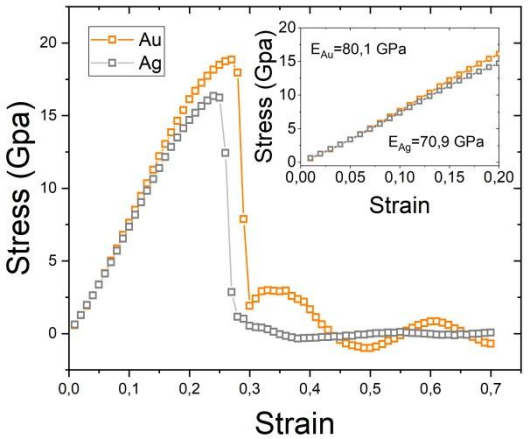

Fig. 4 – Strain-stress curves for Au and Ag nanowires. Inset shows the region of the elastic deformation

Young moduli, estimated from elastic parts of strain-stress curves are equal to $E = 80.1$ GPa and $E = 70.9$ GPa for gold and silver nanorods, respectively. Obtained values are in good agreement with similar data obtained from MD simulations [5, 13, 14].

Atomistic configurations of the Au and Ag samples at different strain are shown in Fig. 5.

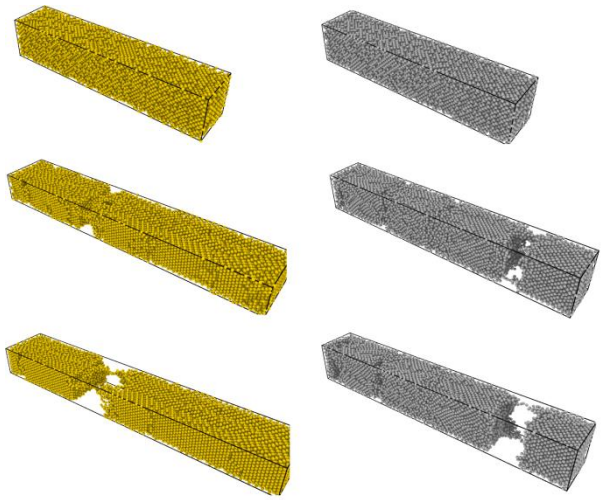

Fig. 5 – Atomic configurations of Au (left) and Ag (right) nanowires at strain of 0.00, 0.54, 0.57 from top to bottom for Au, and 0.00, 0.39, 0.43 from top to bottom for Ag

As can be seen from the figure, the crystalline structure with a face-centered cubic lattice is preserved in most parts of the samples, while the regions of the amorphous state are formed in the area of fracture for both Au and Ag nanorods. However, in contrast to the Au@Ag core-shell nanorod, for Au and Ag samples the prior fracture necking was not observed. This may be due to a different shape of the studied nanorods and slightly different strain ratio.

It is also worth to mention that the plastic deformation and fracture of the Ag and Au samples are developed in different scenarios. Thus, for silver nanorod after the point of yield stress several regions of plastic deformation appear along the sample (Fig. 6).

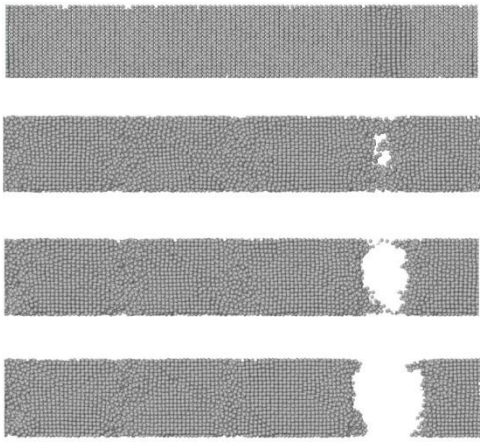

Fig. 6 – Failure dynamics of the Ag nanorod under tensile deformation. Snapshots are taken at strain of 0.35, 0.39, 0.43 and 0.46 from top to bottom

At larger strain, a single fracture is formed in one of these regions, which leads to the destruction of the sample and relaxation of the mechanical stresses. However, the plastic regions are not relaxed to the initial FCC structure (bottom panel in Fig. 6).

In contrast to this, gold nanorod is characterized by a single region of the plastic deformation (see Fig. 7), which became the point of fracture at larger strains. Since both Au and Ag samples have the similar sizes and were simulated under the same conditions, the difference in failure dynamics is more likely caused by different strength of interatomic forces in gold and silver.

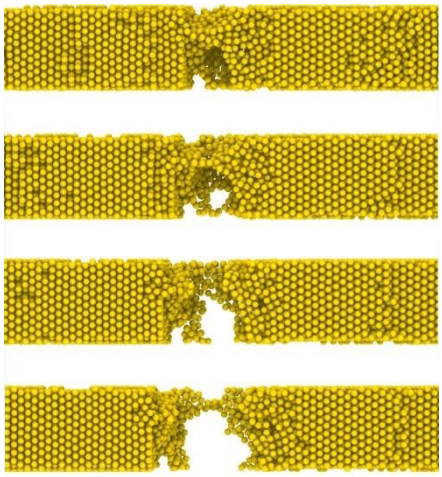

Fig. 7 – Failure dynamics of the Au nanorod under tensile deformation. Snapshots are taken at strain of 0.50, 0.54, 0.57 and 0.60 from top to bottom

4. CONCLUSIONS

We reported the results of numerical simulation by classical molecular dynamics of the mechanical properties of Au, Ag, and bimetallic core-shell Au@Ag nanorods at tensile deformation. Mechanical properties of Au@Ag nanorod were studied using developed computer code for parallel calculations, while pristine Au and Ag samples were studied using the well-known software package. As a result of modeling, mechanical parameters of the samples, such as the elastic moduli, were calculated. The obtained values are equal to $E \approx 57.3$ GPa, $E \approx 80.1$ GPa and $E \approx 70.9$ GPa for Au@Ag, Au and Ag samples, respectively. Also, analysis of the snapshots of atomistic configurations shows that considered samples are characterized by different failure dynamics. Thus, necking was observed for Au@Ag core-shell nanorod, while the pristine Ag sample is characterized by several regions of plastic deformation. At the same time, for Au nanorod a single region of plastic deformation and failure was observed. Even though we used the same interatomic potential for Au@Ag and gold and silver nanorods, obtained results significantly differ for bimetallic and pristine samples. The sufficient difference between the obtained data for core-shell and pristine samples can be explained by several factors. Besides chemical composition and structural difference, size and shape of the samples also may play an important role in experiment. Moreover, in presented work, two types of boundary conditions were used: free for Au@Ag nanorod and periodic for Au and Ag samples, which may also affect the results.

It is worth to recall that measuring elastic parameters of metallic nanostructures in experiments may present a very hard challenge, and requires special

laboratory conditions and equipment. Thus, computer simulations may become a very useful option. Nevertheless, as it was mentioned earlier, general mechanical parameters obtained from MD simulations may depend on many factors, such as size and shape of the samples, boundary conditions, interatomic potential, strain rate and others. Therefore, obtained in this work elastic moduli can be considered only as approximate values, which need to be confirmed later by experimental techniques or other calculations.

ACKNOWLEDGEMENTS

VB and BN are grateful to the Ministry of Education and Science of Ukraine for financial support (Project No. 0117U003923).

REFERENCES

1. R.G. Chaudhuri, S. Paria, Chem. Rev. **112**, 2373 (2012).
2. J.H. Song, F. Kim, D. Kim, P. Yang. *Chem. Eur. J.* **11**, 910 (2005).
3. M. Tsuji, N. Miyamae, S. Lim, K. Kimura, X. Zhang, S. Hikino, M. Nishio, Cryst. Growth. Des. **6**, 1801 (2006).
4. S.J.A. Koh, H.P. Lee, *Nanotechnology* **17**, 3451 (2006).
5. H.S. Park, J.A. Zimmerman, *Phys. Rev. B.* **72**, 054106 (2005).
6. X.W. Zhou, H.N.G. Wadley, R.A. Johnson, D.J. Larson, N. Tabat, A. Cerezo, A.K. Petford-Long, G.D.W. Smith, P.H. Clifton, R.L. Martens, T.F. Kelly, *Acta Mater.* **49**, 4005 (2001).
7. V. Borysiuk, I. Lyashenko, *IEEE 36th International Conference on Electronics and Nanotechnology (ELNANO-2016),* 118 (Kyiv: 2016).
8. V.M. Borysiuk, U.S. Shvets, *NAP-2016, 6th International Conference on Nanomaterials: Applications and Properties (NAP),* 01NNPT04 (Lviv: 2016).
9. S.J. Mejía-Rosales, C. Fernández-Navarro, E. Pérez-Tijerina, J.M. Montejano-Carrizales, M. José-Yacamán, *J. Phys. Chem. B* **110**, 12884 (2006).
10. D.H. Tsai. *J. Chem. Phys.* **70** No 3, 1375 (1979).
11. H.J.C. Berendsen, J.P.M Postma, W.F. van Gunsteren, A. DiNola, J.R. Haak, *J. Chem. Phys.* **81** No8, 3684 (1984).
12. S. Plimpton, *J. Comput. Phys.* **117** No 1, 1 (1995).
13. K. Gall, J. Diao, M.L. Dunn, *Nano Lett.* **4** No 12, 2431 (2004).
14. W. Wang. Ch. Yi, B. Ma, *Proc. IMechE Part N: J Nanoengineering and Nanosystems* **227** No 3, 135 (2013).

Пружні властивості Au, Ag і біметалевих Au@Ag нанодротів з моделювання методами молекулярної динаміки

У. Швець, Б. Наталіч, В. Борисюк

Сумський державний університет, вул. Римського-Корсакова, 2, 40007 Суми, Україна

Наведено результати моделювання механічних властивостей нанодротів золота, срібла та біметалевого Au@Ag зі структурою ядро-оболонка. Досліджено динамічну поведінку зразків під час деформації розтягування в рамках класичної молекулярної динаміки. Взаємодії між атомами в зразках описані за допомогою методу зануреного атому (EAM) та моделі сплаву EAM для взаємодії золото-срібло в структурі ядро-оболонка Au@Ag. Для вивчення механічних властивостей нанодротів до зразків була застосована процедура деформації розтягування. Розтягування зразків реалізувалося шляхом зміщення нерухомих атомів, розташованих у двох зовнішніх атомних шарах на протилежних бічних поверхнях зразків один від одного за постійної швидкості деформації 0.004 пс$^{-1}$. Температуру зразків підтримували на рівні 300 K упродовж усього часу моделювання, використовуючи термостат Берендсена. У процесі деформації для кожного зразка були розраховані механічні напруження в рамках теореми віріалу та побудовані криві навантажень. Одержані криві навантажень мають типову форму з лінійною ділянкою на початку і подальшою нелінійною частиною, що відповідає пластичній деформації. Модулі Юнга досліджуваних зразків оцінювались шляхом лінійної регресії пружної частини кривих деформаційних напружень. Одержані значення дорівнюють 57.3 ГПа, 80.1 ГПа, 70.9 ГПа для зразків Au@Ag, Au і Ag відповідно. Аналіз знімків атомістичних конфігурацій показує, що розглянуті зразки характеризувалися різним характером розриву.

Ключові слова: Молекулярна динаміка, Нанодріт, Ядро-оболонка, Модуль.